

Prospects for discovering strongly decaying doubly heavy T_{bc} tetraquark states at LHCb

Mingjie Feng,^{1,2} Yiming Li,^{1,*} and Hua-Sheng Shao³

¹*Institute of High Energy Physics, Chinese Academy of Science, Beijing 100049, China*

²*University of Chinese Academy of Science, Beijing 100049, China*

³*Laboratoire de Physique Théorique et Hautes Energies (LPTHE), UMR 7589, Sorbonne Université et CNRS, 4 place Jussieu, 75252 Paris, France*

(Dated: January 21, 2026)

We investigate the discovery potential of the T_{bc} states with $J^P = 0^+$ in proton-proton (pp) collisions at LHCb at a center-of-mass energy of $\sqrt{s} = 13$ TeV. The study focuses on the decay channel $T_{bc} \rightarrow B^- D^+$. A phenomenological approach is employed to construct the background model based on the associated production of B and D mesons, incorporating previously published LHCb results. Background processes are simulated using `MadGraph5_aMC@NLO` and `Pythia8.3`. We explore the parameter space of the T_{bc} mass, width, production cross section, and the effective double-parton-scattering cross section (σ_{eff}) relevant for the BD meson background. The integrated luminosity required for a 5σ discovery at LHCb is evaluated under various assumptions. We find that a 5σ observation is achievable for a production cross section of 103 nb, which is expected to be within reach during Run 4. In addition, we estimate the minimum observable $\sigma(T_{bc}) \times \mathcal{B}(T_{bc} \rightarrow B^- D^+)$ for a 5σ discovery under different luminosity scenarios, providing guidance for future experimental searches at LHCb.

I. INTRODUCTION

Since the discovery of the $X(3872)$ by the Belle experiment in 2003 [1], several resonant states have been observed that cannot be accommodated within the conventional quark-model description of the hadron spectrum. Their observation has significantly broadened our understanding of hadron spectroscopy. Exotic hadrons also play an important role in the study of quantum chromodynamics (QCD), as they provide a unique window into the non-perturbative dynamics of the strong interaction. As a result, the investigation of exotic hadronic states has become one of the frontiers of hadron physics over the past two decades. A wide variety of theoretical models have been proposed, accompanied by extensive experimental efforts to search for new exotic states through different production mechanisms and to measure their masses, widths, production cross sections, and spin-parity quantum numbers in order to elucidate their internal structure.

Numerous theoretical predictions exist for the ground-state mass of the $T_{bc}(bc\bar{u}\bar{d})$ tetraquark (Charge conjugation is implied throughout this paper). The T_{bc} mass is generally expected to lie close to the threshold of an open-bottom and an open-charm meson. The predicted mass difference with respect to the $\bar{B}D$ threshold falls in the range [2–11]

$$-50 \text{ MeV} < m(T_{bc}) - m(\bar{B}) - m(D) < 120 \text{ MeV}. \quad (1)$$

At present, it remains unclear whether the T_{bc} mass lies above or below the $\bar{B}D$ threshold. If the mass lies below threshold, the T_{bc} would be stable against strong de-

cays and could only be accessed via weak interactions [2–7]. If the mass lies above threshold, the T_{bc} is expected to appear as a relatively narrow resonance in the $\bar{B}D$ invariant-mass spectrum and can therefore be searched for directly [8–11]. In this study, we focus on the latter scenario, where the T_{bc} lies above the threshold and can be identified through its narrow resonance in the $\bar{B}D$ invariant-mass spectrum. Studies of heavy-flavor hadron-associated production thus provide a powerful experimental avenue for the discovery of new hadronic states containing different heavy quarks.

From the perspective of production mechanisms, associated BD production proceeds primarily through single-parton scattering (SPS) and multiparton scattering (DPS). The latter is dominated by double-parton scattering (DPS), while contributions from higher-order multiparton interactions are expected to be suppressed. The relative importance of DPS is expected to increase with increasing proton-proton collision energy. Studies of associated BD production provide a sensitive probe of heavy-flavor production mechanisms, enable quantitative tests of SPS and DPS dynamics (see, e.g., ref. [12]), constrain heavy-quark correlations and fragmentation, and supply essential background information for searches for exotic states such as the T_{bc} tetraquark.

The observation of the doubly charmed tetraquark T_{cc}^+ by the LHCb Collaboration in 2021, reconstructed in the $D^0 D^0 \pi^+$ final state [13], has demonstrated the feasibility of searching for multiquark states with multiple heavy flavors through associated heavy-flavor production. Owing to the high heavy-flavor production rate in pp collisions, its excellent vertexing and tracking capability, efficient trigger, and precise control of detector-induced asymmetries, the LHCb experiment provides an ideal environment for searches for the T_{bc} .

The $T_{bc}(bc\bar{u}\bar{d})$ tetraquark with quantum numbers

* liyiming@ihep.ac.cn

$J^P = 0^+$ are expected to decay strongly into $\bar{B}^0 D^0$, $B^- D^+$, and their charge-conjugate modes if the mass is above the meson-pair thresholds. This analysis investigates the experimental potential of the LHCb experiment to discover the T_{bc} through its production and decay into BD meson pairs. The study focuses on the decay chain

$$\begin{aligned} T_{bc} &\rightarrow B^- D^+, \\ B^- &\rightarrow J/\psi (\rightarrow \mu^+ \mu^-) K^-, \\ D^+ &\rightarrow K^- \pi^+ \pi^+, \end{aligned} \quad (2)$$

which provides a clean experimental signature for the discovery of the T_{bc} at LHCb.

II. METHOD

A. Background Simulations

In this analysis, both SPS and DPS processes are considered as the dominant mechanisms contributing to the background in the $B^\mp D^\pm$ final state for the T_{bc} search. The background samples for the two processes are generated separately, with the DPS sample reweighted to reproduce the differential distributions observed in LHCb. The following kinematic selection cuts are applied to both background samples to reflect the LHCb detector acceptance:

$$\begin{aligned} 2.0 < y_{B/D} < 4.5, \\ p_{T,B} < 40 \text{ GeV}, \\ 1 \text{ GeV} < p_{T,D} < 8 \text{ GeV}. \end{aligned} \quad (3)$$

The SPS and DPS background samples are generated using `MadGraph5_aMC@NLO` (`MG5_aMC` hereafter) [14, 15], with parton showering and hadronization performed by `Pythia8.3` [16]. We consider proton-proton collisions at $\sqrt{s} = 13$ TeV. The charm- and bottom-quark masses are set to $m_c = 1.55$ GeV and $m_b = 4.7$ GeV, respectively. The `NNPDF2.3` parton distribution functions (PDFs) [17] are employed, with next-to-leading order (NLO) PDFs used for NLO simulations and leading order (LO) PDFs for LO simulations. Both the renormalization and factorization scales are chosen dynamically, with the central value given by $\mu_0 = H_T/2$, where H_T is the scalar sum of the transverse energies of the final-state particles.

For simulating the SPS background, we consider two complementary approaches to generate samples. First, we study the process $pp \rightarrow b\bar{b}c\bar{c} + X$ in the 3-flavor number scheme (3FNS) at NLO in QCD, with matching to parton showers performed using the `MC@NLO` method [18]. We take the 3FNS calculation as the nominal prediction. The corresponding fiducial cross section, with fiducial cuts given in eq. (3), is found to be

$$\sigma_{B^\mp D^\pm}^{\text{NLO SPS 3FNS}} = 0.074^{+0.040}_{-0.034} \text{ } \mu\text{b}, \quad (4)$$

where the uncertainty arises mainly from variations of the renormalization and factorization scales. The fiducial cross section includes both $B^- D^+$ and $B^+ D^-$ final

states. Together with the DPS contribution, this NLO SPS prediction defines the *baseline background scenario* used to assess the T_{bc} discovery potential.

Alternatively, as discussed in ref. [19], the resummation of initial-state logarithms arising from gluon splitting into a charm-quark pair may be crucial to describe the LHCb $J/\psi + D$ measurement [20]. We therefore additionally generate the SPS sample at LO with charm- or anticharm-gluon initial states in the 4-flavor number scheme (4FNS). This LO 4FNS calculation yields a fiducial cross section of

$$\sigma_{B^\mp D^\pm}^{\text{LO SPS 4FNS}} = 0.21^{+0.44}_{-0.15} \text{ } \mu\text{b}, \quad (5)$$

where the dominant theoretical uncertainty originates from scale variations. Similar to the $J/\psi + D$ case [19], the 4FNS calculation significantly enhances the SPS fiducial cross section compared to the 3FNS result. To obtain a conservative estimate of the T_{bc} discovery potential under a maximal background assumption, we take the 1σ upper bound of the LO SPS 4FNS prediction, $\sigma_{B^\mp D^\pm, \text{max}}^{\text{LO SPS 4FNS}} = 0.65 \text{ } \mu\text{b}$, and combine it with the DPS contribution. This defines the *conservative maximal-background scenario*.

To simulate the DPS background, two NLO event samples for the processes $pp \rightarrow b\bar{b} + X$ and $pp \rightarrow c\bar{c} + X$ are generated separately. The DPS BD sample is obtained by randomly pairing events from the single- B^\mp and single- D^\pm samples. In the DPS approximation, the kinematic properties of the B and D mesons are largely governed by their respective single-particle distributions. However, the single-particle rapidity spectra predicted by `MG5_aMC` may differ from those observed in data. To reduce this model dependence, the DPS sample is reweighted event-by-event according to the rapidity difference $\Delta y = y_B - y_D$, using a reference Δy distribution constructed from the LHCb Run 2 measurements of the single-particle $d\sigma/dy$ spectra of B and D mesons [21, 22], as illustrated in Fig. 1.

The total fiducial cross section of the DPS process is

$$\sigma_{B^\mp D^\pm}^{\text{DPS}} = \frac{1}{2} \times \frac{\sigma_{B^\mp} \cdot \sigma_{D^\pm}}{\sigma_{\text{eff}}} = \left(\frac{15 \text{ mb}}{\sigma_{\text{eff}}} \right) (2.4 \pm 0.3 \text{ } \mu\text{b}), \quad (6)$$

where $\sigma_{B^\mp} = 86.6 \pm 6.4 \text{ } \mu\text{b}$ [21] and $\sigma_{D^\pm} = 834 \pm 78 \text{ } \mu\text{b}$ [22], measured using the same fiducial cuts as in eq. (3). The factor of 1/2 accounts for the fact that only the charge-neutral combinations $B^- D^+$ and $B^+ D^-$ are considered, since σ_{B^\mp} and σ_{D^\pm} include charge-conjugate contributions. The effective DPS cross section σ_{eff} is not precisely known but has been extracted from LHCb measurements of other heavy-flavor processes, such as $\Upsilon + D$ [23], $J/\psi + \Upsilon$ [24], and $J/\psi + D$ [19, 20], with typical values in the range 5-30 mb. In this analysis, we consider representative values $\sigma_{\text{eff}} = 5, 15$, and 30 mb .

Differential cross sections for $B^\mp D^\pm$ associated production via the SPS, DPS, and combined SPS+DPS mechanisms are shown in Fig. 2. The upper panels correspond to the SPS prediction obtained at NLO in the

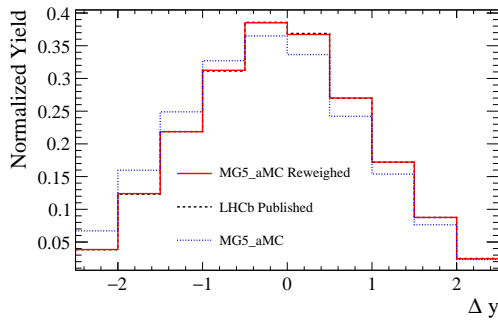


FIG. 1. Comparison of the rapidity difference Δy between the B^\mp and D^\pm mesons for the DPS background. The black dashed line represents published LHCb Run 2 data, while the red solid and blue dotted lines correspond to the reweighted and unweighted DPS simulations, respectively. Results are shown for $\sigma_{\text{eff}} = 15$ mb.

3FNS, while the lower panels show the LO SPS prediction in the 4FNS. The shaded bands indicate the combined statistical and systematic uncertainties. For both SPS and DPS, statistical uncertainties are estimated from the event samples. The DPS systematic uncertainty arises from σ_{B^\mp} and σ_{D^\pm} , while the SPS systematic uncertainties are dominated by variations of the renormalization and factorization scales in the perturbative calculations.

The azimuthal angle difference distribution, $\Delta\phi = |\phi(B) - \phi(D)|$, in the SPS mechanism exhibits a prominent peak near π , indicating that B^\mp and D^\pm mesons are predominantly produced in a back-to-back configuration in the transverse plane. In contrast, the DPS mechanism yields a nearly uniform $\Delta\phi$ distribution, reflecting the absence of strong azimuthal correlations between the two mesons. Similarly, the rapidity gap Δy distinct features for the two mechanisms. SPS events produce an asymmetric Δy distribution, with the B meson typically more central in rapidity than the D meson, whereas DPS events result in a nearly symmetric distribution around $\Delta y = 0$, consistent with the largely uncorrelated production of the two mesons. The invariant mass distribution $M(B^\mp D^\pm)$ further highlights these differences. SPS events, dominated by back-to-back configurations, lead to a relatively broad distribution with a pronounced high-mass tail, while DPS events produce a narrower peak, although occasional high-momentum combinations can generate a small tail. Overall, these observables illustrate the distinct kinematic patterns of the SPS and DPS mechanisms and provide multiple handles for disentangling their respective contributions.

Within the LHCb kinematic acceptance, associated $B^\mp D^\pm$ production is dominated by the DPS mechanism when using the nominal NLO SPS prediction in the 3FNS, for which the SPS contribution is negligible. Only when adopting the conservative upper-bound LO SPS calculation in the 4FNS does the SPS contribution become comparable to DPS in certain kinematic regions.

These differential distributions, based on the kinematic

cuts defined in eq. (3), will be used as the background for the T_{bc} search in subsequent analyses.

B. Generation of the T_{bc} Signal

In this analysis, the generation of the T_{bc} signal assumes specific values of its mass $m(T_{bc})$, width $\Gamma(T_{bc})$, and production cross section $\sigma(T_{bc})$, motivated by theoretical expectations. Signal samples are generated for different mass and width hypotheses. The T_{bc} signal is modeled using a Breit–Wigner (BW) distribution to describe its natural width, which is subsequently convolved with the detector response function to obtain the differential cross-section distribution.

The differential cross section for T_{bc} production can be written as

$$\frac{d\sigma_{T_{bc}}}{dm} = \sigma(T_{bc}) \int_{-\infty}^{+\infty} \text{BW}(m') \cdot G(m - m', \sigma_{\text{res}}) dm', \quad (7)$$

where $\sigma(T_{bc}) \equiv \sigma(pp \rightarrow T_{bc} + X) + \sigma(pp \rightarrow \bar{T}_{bc} + X)$ denotes the total inclusive production cross section of the T_{bc} and \bar{T}_{bc} states, without applying any fiducial cuts, and $m \equiv M(B^\mp D^\pm)$ is the invariant mass of the reconstructed $B^\mp D^\pm$ pair. The non-relativistic BW distribution is given by

$$\text{BW}(m') = \frac{1}{2\pi} \frac{\Gamma(T_{bc})}{(m' - m(T_{bc}))^2 + (\Gamma(T_{bc})/2)^2}. \quad (8)$$

The detector response function G is modeled by a Gaussian distribution:

$$G(m - m', \sigma_{\text{res}}) = \frac{1}{\sqrt{2\pi}\sigma_{\text{res}}} \exp \left[-\frac{(m - m')^2}{2\sigma_{\text{res}}^2} \right], \quad (9)$$

motivated by LHCb measurements of similar decay modes, such as $B_c^+ \rightarrow J/\psi D_s^+$ and $B_c^+ \rightarrow B_s^0 (\rightarrow D_s^-\pi^+)\pi^+$ [25], for which the mass resolution is found to be in the range 4–7 MeV. Given that the $T_{bc} \rightarrow B^- D^+$ decay chain, eq. (2), involves multiple tracks and allows for intermediate mass constraints, we adopt a mass resolution of $\sigma_{\text{res}} = 6$ MeV in the simulation.

In this study, we consider two representative mass hypotheses for the T_{bc} , $m(T_{bc}) = 7167$ MeV and $m(T_{bc}) = 7229$ MeV, motivated by theoretical predictions for exotic hadron states with quantum numbers $J^P = 0^+$ [9, 10]. These values correspond to possible T_{bc} configurations and span a reasonable range consistent with current theoretical expectations for heavy tetraquarks. For these mass hypotheses, we consider several representative values of the width and production cross section. The width values $\Gamma(T_{bc}) = 0.5, 5$ MeV are used for $m(T_{bc}) = 7167$ MeV, while $\Gamma(T_{bc}) = 10, 40$ MeV are adopted for $m(T_{bc}) = 7229$ MeV. These choices are motivated by comparisons with similar exotic hadrons: the narrow width of the T_{cc}^+ ($\Gamma(T_{cc}^+) \sim 0.4$ MeV) [13], and the broader widths of states such as $Z_c(3900)$ and $Z_b(10610)$, which have widths of order 10–30 MeV [26, 27].

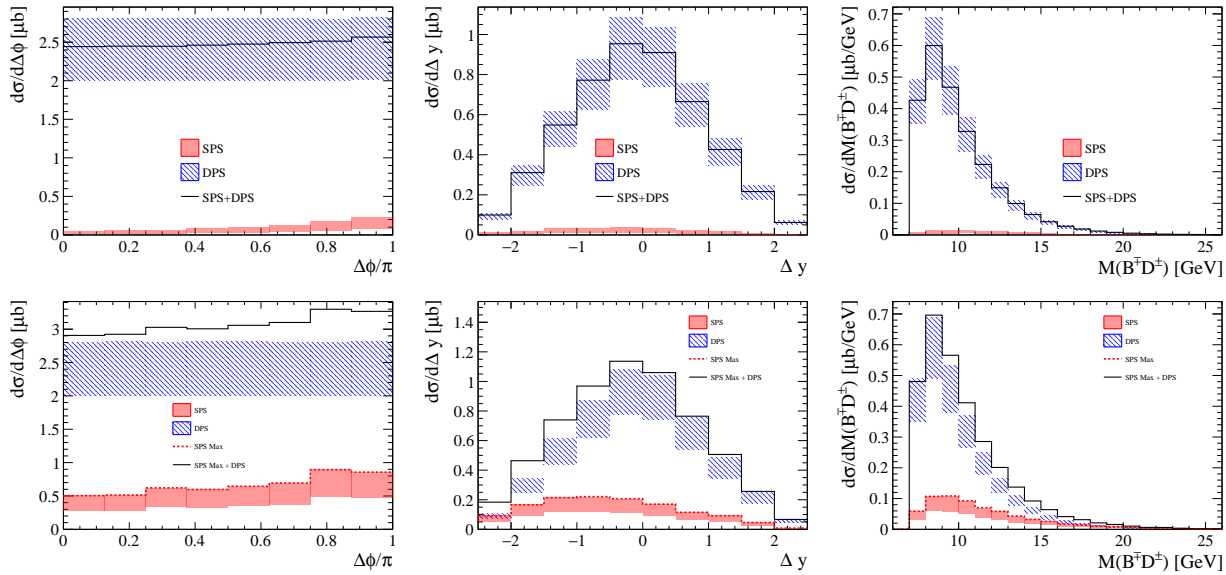


FIG. 2. Differential cross sections for associated $B^\mp D^\pm$ production via SPS and DPS mechanisms. Left: $\Delta\phi$ distribution; middle: Δy distribution; right: invariant mass $M(B^\mp D^\pm)$ distribution, shown for $\sigma_{\text{eff}} = 15 \text{ mb}$. The upper (lower) panels correspond to the SPS prediction obtained at NLO in the 3FNS (LO in the 4FNS). The SPS contribution is shown as a red shaded band, with uncertainties dominated by renormalization and factorization scale variations, while the DPS contribution is shown as a blue hatched band. In the upper panels, the black solid line denotes the combined SPS+DPS central prediction, defining the baseline background scenario. In the lower panels, the red dashed line indicates the maximal SPS contribution obtained from the upper bound of the LO 4FNS prediction, while the black solid line shows the corresponding SPS (max)+DPS prediction, defining the conservative maximal background scenario.

For the production cross section, we take $\sigma(T_{bc}) = 103 \text{ nb}$ as the baseline, motivated by theoretical predictions at $\sqrt{s} = 13 \text{ TeV}$ [28]. To assess the discovery potential, we scan over different values of $\sigma(T_{bc}) \times \mathcal{B}(T_{bc} \rightarrow B^- D^+)$ for selected integrated luminosities, and evaluate how variations in the assumed production cross section impact the observability of the T_{bc} signal.

Based on these assumptions, we generate the T_{bc} signal and evaluate the discovery potential for different parameter combinations. Since the T_{bc} resonance is narrow and the background is largely smooth in the $B^\mp D^\pm$ invariant mass spectrum, signal-background interference is expected to be small. In particular, the interference effect decreases with decreasing signal width $\Gamma(T_{bc})$, and can be safely neglected for the narrowest widths considered ($\Gamma(T_{bc}) = 0.5 \text{ MeV}$). Therefore, we do not include the signal-background interference in our study.

C. Signal and Background Yields

In this analysis, after constructing the signal and background cross-section distributions, the number of signal and background events is estimated based on the decay chain in eq. (2). The event yields for both signal and background are calculated using the standard formula for event counting:

$$N = \sigma \times \mathcal{L}_{\text{int}} \times \mathcal{B} \times \varepsilon, \quad (10)$$

where

- σ represents the production cross section. For the signal, $\sigma = \sigma(T_{bc})$, while for the background it is given by the sum of the SPS and DPS contributions: $\sigma = \sigma_{B^\mp D^\pm}^{\text{DPS}} + \sigma_{B^\mp D^\pm}^{\text{SPS}}$. In this study, we neglect the dependence of σ on the pp center-of-mass energy between 13 TeV and 14 TeV.
- \mathcal{L}_{int} is the integrated luminosity. LHCb has already collected approximately 6 fb^{-1} of pp collision data during Run 2 at $\sqrt{s} = 13 \text{ TeV}$. The Run 1 dataset is not included in this study, as its relatively small integrated luminosity and lower center-of-mass energies (7 and 8 TeV) contribute negligibly to the overall sensitivity. By the end of Run 4, the total integrated luminosity from Run 2, Run 3, and Run 4 is expected to reach $\sim 50 \text{ fb}^{-1}$, and by the end of Run 5, $\sim 300 \text{ fb}^{-1}$. Therefore, in this study, we scan \mathcal{L}_{int} in the range of $5\text{--}300 \text{ fb}^{-1}$.
- \mathcal{B} represents the total branching ratio. The relevant values are $\mathcal{B}(B^\pm \rightarrow J/\psi K^\pm) = (1.020 \pm 0.019) \times 10^{-3}$, $\mathcal{B}(D^\pm \rightarrow K^\mp \pi^\pm \pi^\pm) = (9.38 \pm 0.16) \times 10^{-2}$, and $\mathcal{B}(J/\psi \rightarrow \mu^+ \mu^-) = (5.961 \pm 0.033) \times 10^{-2}$ [29]. For the signal decay $T_{bc} \rightarrow B^- D^+$, we assume a branching fraction $\mathcal{B}(T_{bc} \rightarrow B^- D^+) = 0.5$ by default.
- ε is the total event reconstruction and selection efficiency, including contributions from detector ge-

ometric acceptance, track reconstruction, trigger, particle identification, and offline selection. For the decay $T_{bc} \rightarrow B^- D^+$, the efficiency is the product $\varepsilon_B \times \varepsilon_D$, with the trigger efficiency for D not included, since the BD candidates are triggered by the B meson. The total efficiency is estimated from measurements of related decays [21, 22], giving $\varepsilon_{BD} = (0.6 \pm 0.3)\%$.

Figure 3 shows an example of the invariant mass spectrum of the reconstructed $B^\mp D^\pm$ pair for an integrated luminosity of 50 fb^{-1} , assuming a T_{bc} production cross section of $\sigma(T_{bc}) = 103 \text{ nb}$ and an effective DPS cross section of $\sigma_{\text{eff}} = 15 \text{ mb}$. In this case, the T_{bc} signal appears as a clear resonance peak at the expected mass.

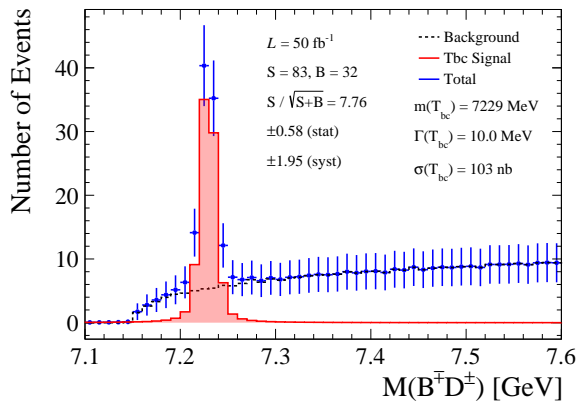


FIG. 3. Combined distribution of the T_{bc} signal and background in the BD invariant-mass spectrum for an effective DPS cross section $\sigma_{\text{eff}} = 15 \text{ mb}$, $m(T_{bc}) = 7229 \text{ MeV}$, and $\Gamma(T_{bc}) = 10 \text{ MeV}$. The black curve represents the associated $B^\mp D^\pm$ background, the red curve the T_{bc} signal, and the blue curve their sum.

D. Discovery Potential

After obtaining the signal and background yields, N_{Sig} and N_{Bkg} , for different parameter assumptions, the significance of the T_{bc} signal is estimated using the standard formula

$$Z = \frac{N_{\text{Sig}}}{\sqrt{N_{\text{Sig}} + N_{\text{Bkg}}}} , \quad (11)$$

where N_{Sig} and N_{Bkg} denote the numbers of signal and background events within a $\pm 3\sigma_{\text{eff res}}$ mass window, evaluated using eq. (10). The effective mass resolution is defined as

$$\sigma_{\text{eff res}} = \sqrt{\left(\frac{\Gamma(T_{bc})}{2.35}\right)^2 + \sigma_{\text{res}}^2} , \quad (12)$$

and the mass window is centered on the signal peak in the invariant $B^\mp D^\pm$ mass spectrum.

In this study, we evaluate the discovery potential of the T_{bc} by scanning the significance Z as a function of integrated luminosity \mathcal{L}_{int} for different T_{bc} mass and width hypotheses, as well as for different values of the effective DPS cross section σ_{eff} contributing to the background. This scan allows us to determine the minimum integrated luminosity required for a 5σ discovery of the T_{bc} under the various assumptions.

In addition, we perform a scan over $\sigma(T_{bc}) \times \mathcal{B}(T_{bc} \rightarrow B^- D^+)$ to evaluate how different assumed signal strengths affect the discovery significance. By calculating Z for various integrated luminosities, we determine the minimum observable $\sigma(T_{bc}) \times \mathcal{B}(T_{bc} \rightarrow B^- D^+)$ corresponding to a 5σ threshold, providing a quantitative assessment of the T_{bc} discovery potential under different experimental conditions.

III. RESULTS

A. Minimum Integrated Luminosity for a 5σ Discovery at LHCb

Figure 4 shows the statistical significance Z of the T_{bc} signal in the BD invariant-mass spectrum as a function of integrated luminosity \mathcal{L}_{int} , for different values of the effective DPS cross section σ_{eff} and for various T_{bc} mass and width assumptions. A baseline background scenario is assumed, together with a production cross section $\sigma(T_{bc}) = 103 \text{ nb}$ and a branching fraction $\mathcal{B}(T_{bc} \rightarrow B^- D^+) = 0.5$. The values of σ_{eff} are set to 5, 15, and 30 mb, from left to right. As σ_{eff} increases, the DPS background cross section decreases, thereby enhancing the discovery potential for T_{bc} . Furthermore, Fig. 5 and Table I present the minimum integrated luminosity required to achieve a 5σ discovery of T_{bc} for different T_{bc} parameter assumptions assuming $\sigma(T_{bc}) = 103 \text{ nb}$ and $\mathcal{B}(T_{bc} \rightarrow B^- D^+) = 0.5$.

These results indicate that, for most T_{bc} parameter sets, a 5σ discovery can be achieved with an integrated luminosity of 50 fb^{-1} (Run 2 + Run 3 + Run 4). This suggests that a systematic search for T_{bc} could be carried out in the near future, with a high likelihood of success during Run 4 data taking. In addition, a comparison between the baseline background scenario and the conservative maximal-background scenario shows that the required integrated luminosity is largely insensitive to the SPS modeling, demonstrating the robustness of the proposed search strategy.

B. Minimum Cross Section times Branching Fraction for a 5σ Discovery of T_{bc} at LHCb

Tables II and III show the minimum observable values of the product $\sigma(T_{bc}) \times \mathcal{B}(T_{bc} \rightarrow B^- D^+)$ required for a 5σ discovery of T_{bc} under different integrated luminosity scenarios. Table II corresponds to $\mathcal{L}_{\text{int}} = 50 \text{ fb}^{-1}$, combining

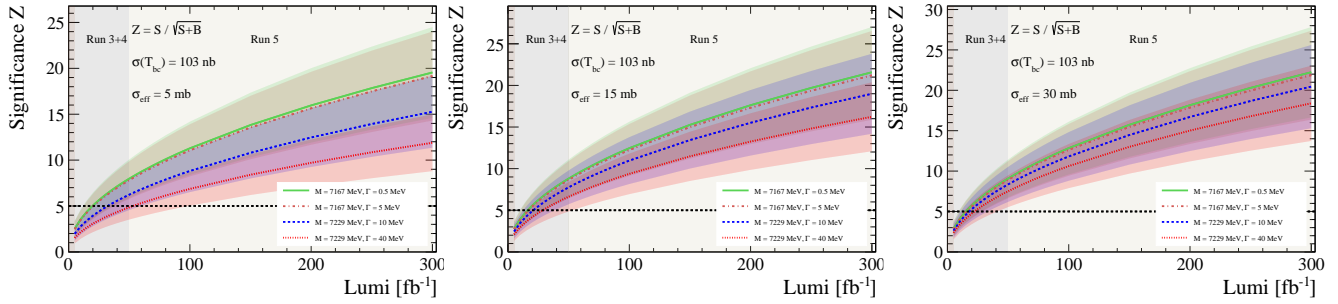


FIG. 4. Statistical significance Z of the T_{bc} signal in the BD invariant-mass spectrum as a function of the integrated luminosity \mathcal{L}_{int} , for different T_{bc} mass and width assumptions and values of the effective DPS cross sections σ_{eff} . A baseline background scenario (DPS + NLO SPS in the 3FNS), a production cross section $\sigma(T_{bc}) = 103 \text{ nb}$, and a branching fraction $\mathcal{B}(T_{bc} \rightarrow B^- D^+) = 0.5$ are assumed. The left, middle, and right panels correspond to $\sigma_{\text{eff}} = 5 \text{ mb}$, 15 mb , and 30 mb , respectively. Different colors denote different T_{bc} mass and width assumptions: $M = 7167 \text{ MeV}$ with $\Gamma = 0.5, 5 \text{ MeV}$, and $M = 7229 \text{ MeV}$ with $\Gamma = 10, 40 \text{ MeV}$, where $M \equiv m(T_{bc})$ and $\Gamma \equiv \Gamma(T_{bc})$. The dashed line indicates the 5σ discovery threshold.

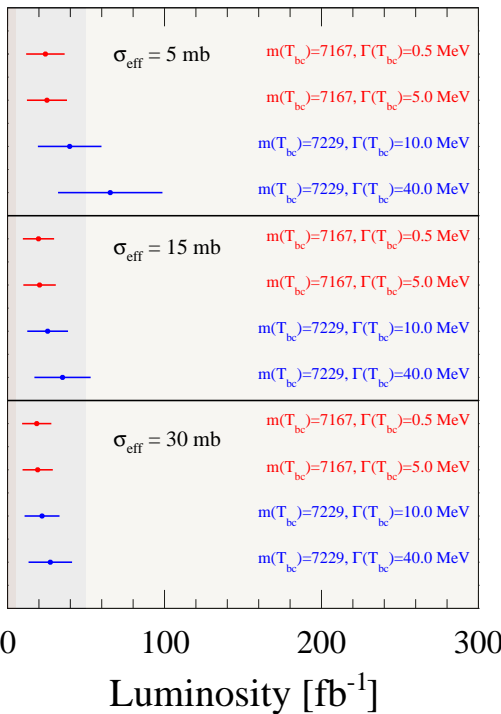


FIG. 5. Discovery significance of T_{bc} as a function of integrated luminosity for different T_{bc} mass and width parameters, assuming the baseline background scenario, $\sigma(T_{bc}) = 103 \text{ nb}$, and $\mathcal{B}(T_{bc} \rightarrow B^- D^+) = 0.5$.

data from Run 2 to Run 4, while Table III corresponds to $\mathcal{L}_{\text{int}} = 300 \text{ fb}^{-1}$, including data from Run 2 through Run 5. Increasing the integrated luminosity from 50 fb^{-1} to 300 fb^{-1} significantly lowers the minimum observable $\sigma(T_{bc}) \times \mathcal{B}(T_{bc} \rightarrow B^- D^+)$, enhancing the statistical sensitivity. In particular, the minimal value is reduced by a factor of 3 or more, depending on the T_{bc} parameter

assumptions and the background scenarios.

Assuming $\sigma(T_{bc}) \times \mathcal{B}(T_{bc} \rightarrow B^- D^+)$ lies in the range $20\text{--}60 \text{ nb}$, a 5σ observation of T_{bc} could be achieved by the end of Run 4. Smaller values, in the range $5\text{--}25 \text{ nb}$, would require the full dataset of Run 5. These results emphasize that both the integrated luminosity and the production cross section times branching fraction are key factors determining the discovery potential.

IV. SUMMARY

In this study, we investigate the discovery potential of the T_{bc} state at the LHCb experiment using a phenomenological approach. The background is modeled with MG5_aMC and Pythia8.3 generators, with simulations tuned to published LHCb measurements. We scan the parameter space of the T_{bc} mass ($7167\text{--}7229 \text{ MeV}$), width ($0.5\text{--}40 \text{ MeV}$), production cross section (baseline $\sigma(T_{bc}) = 103 \text{ nb}$), and the effective DPS cross section ($\sigma_{\text{eff}} = 5, 15, 30 \text{ mb}$) to determine the integrated luminosity required for a 5σ discovery. Our results indicate that, for a production cross section of $\sigma(T_{bc}) = 103 \text{ nb}$ and a branching fraction of $\mathcal{B}(T_{bc} \rightarrow B^- D^+) = 0.5$, a 5σ discovery is expected by the end of Run 4, except in the case of a heavy, broad T_{bc} state ($m_{T_{bc}} = 7229 \text{ MeV}$, $\Gamma(T_{bc}) = 40 \text{ MeV}$) with a large DPS background ($\sigma_{\text{eff}} = 5 \text{ mb}$), for which the significance is nevertheless still sizable.

We also evaluated the minimum observable $\sigma(T_{bc}) \times \mathcal{B}(T_{bc} \rightarrow B^- D^+)$ required for a 5σ discovery under different integrated luminosity scenarios. With 50 fb^{-1} of data (Run 2 to Run 4), a discovery is expected if $\sigma(T_{bc}) \times \mathcal{B}(T_{bc} \rightarrow B^- D^+)$ lies between 20 nb and 60 nb . For smaller cross sections in the range 5 nb to 25 nb , the full Run 5 dataset (300 fb^{-1}) is needed.

In conclusion, a systematic search for the T_{bc} at LHCb is feasible, with promising discovery prospects during Run 3 and Run 4. These results provide quantitative

guidance for future experimental searches by defining the integrated luminosity and cross-section thresholds required for a 5σ observation, and pave the way for further exploration of exotic hadrons at LHCb.

ACKNOWLEDGMENTS

We are grateful to Xiaojie Jiang and Xuhao Yuan for useful discussions. The work of MF and YL is supported

by the National Natural Science Foundation of China (NSFC) (grant No.12175245, 12188102, W2443008). The work of HSS is supported by the European Research Council (grant No.101041109, “BOSON”) and the French National Research Agency (grant ANR-20-CE31-0015, “PrecisOnium”). Views and opinions expressed are however those of the authors only and do not necessarily reflect those of the European Union or the European Research Council Executive Agency. Neither the European Union nor the granting authority can be held responsible for them.

-
- [1] **Belle** Collaboration, S. K. Choi *et al.*, “Observation of a narrow charmonium-like state in exclusive $B^\pm \rightarrow K^\pm \pi^\pm J/\psi$ decays,” *Phys. Rev. Lett.* **91** (2003) 262001, [arXiv:hep-ex/0309032](https://arxiv.org/abs/hep-ex/0309032).
- [2] W. Chen, T. G. Steele, and S.-L. Zhu, “Exotic open-flavor $bc\bar{q}\bar{q}$, $bc\bar{s}\bar{s}$ and $qc\bar{q}\bar{l}$, $sc\bar{s}\bar{b}$ tetraquark states,” *Phys. Rev. D* **89** no. 5, (2014) 054037, [arXiv:1310.8337 \[hep-ph\]](https://arxiv.org/abs/1310.8337).
- [3] M. Karliner and J. L. Rosner, “Discovery of doubly-charmed Ξ_{cc} baryon implies a stable $(bb\bar{u}\bar{d})$ tetraquark,” *Phys. Rev. Lett.* **119** no. 20, (2017) 202001, [arXiv:1707.07666 \[hep-ph\]](https://arxiv.org/abs/1707.07666).
- [4] T. F. Caramés, J. Vijande, and A. Valcarce, “Exotic $bc\bar{q}\bar{q}$ four-quark states,” *Phys. Rev. D* **99** no. 1, (2019) 014006, [arXiv:1812.08991 \[hep-ph\]](https://arxiv.org/abs/1812.08991).
- [5] A. Radhakrishnan, M. Padmanath, and N. Mathur, “Study of the isoscalar scalar $bc\bar{u}\bar{d}$ tetraquark T_{bc} with lattice QCD,” *Phys. Rev. D* **110** no. 3, (2024) 034506, [arXiv:2404.08109 \[hep-lat\]](https://arxiv.org/abs/2404.08109).
- [6] S. Meinel, M. Pflaumer, and M. Wagner, “Search for $\bar{b}b\bar{s}\bar{s}$ and $\bar{b}\bar{c}u\bar{d}$ tetraquark bound states using lattice QCD,” *Phys. Rev. D* **106** no. 3, (2022) 034507, [arXiv:2205.13982 \[hep-lat\]](https://arxiv.org/abs/2205.13982).
- [7] W.-L. Wu, Y. Ma, Y.-K. Chen, L. Meng, and S.-L. Zhu, “Doubly heavy tetraquark bound and resonant states,” *Phys. Rev. D* **110** no. 9, (2024) 094041, [arXiv:2409.03373 \[hep-ph\]](https://arxiv.org/abs/2409.03373).
- [8] D. Ebert, R. N. Faustov, V. O. Galkin, and W. Lucha, “Masses of tetraquarks with two heavy quarks in the relativistic quark model,” *Phys. Rev. D* **76** (2007) 114015, [arXiv:0706.3853 \[hep-ph\]](https://arxiv.org/abs/0706.3853).
- [9] E. J. Eichten and C. Quigg, “Heavy-quark symmetry implies stable heavy tetraquark mesons $Q_i Q_j \bar{q}_k \bar{q}_l$,” *Phys. Rev. Lett.* **119** no. 20, (2017) 202002, [arXiv:1707.09575 \[hep-ph\]](https://arxiv.org/abs/1707.09575).
- [10] J.-B. Cheng, S.-Y. Li, Y.-R. Liu, Z.-G. Si, and T. Yao, “Double-heavy tetraquark states with heavy diquark-antiquark symmetry,” *Chin. Phys. C* **45** no. 4, (2021) 043102, [arXiv:2008.00737 \[hep-ph\]](https://arxiv.org/abs/2008.00737).
- [11] Y. Song and D. Jia, “Mass spectra of doubly heavy tetraquarks in diquark–antidiquark picture,” *Commun. Theor. Phys.* **75** no. 5, (2023) 055201, [arXiv:2301.00376 \[hep-ph\]](https://arxiv.org/abs/2301.00376).
- [12] R. Maciula and A. Szczurek, “Double-parton scattering effects in $D^0 B^+$ and $B^+ B^+$ meson-meson pair production in proton-proton collisions at the LHC,” *Phys. Rev. D* **97** no. 9, (2018) 094010, [arXiv:1803.01198 \[hep-ph\]](https://arxiv.org/abs/1803.01198).
- [13] **LHCb** Collaboration, R. Aaij *et al.*, “Observation of an exotic narrow doubly charmed tetraquark,” *Nature Phys.* **18** no. 7, (2022) 751–754, [arXiv:2109.01038 \[hep-ex\]](https://arxiv.org/abs/2109.01038).
- [14] J. Alwall, R. Frederix, S. Frixione, V. Hirschi, F. Maltoni, O. Mattelaer, H. S. Shao, T. Stelzer, P. Torrielli, and M. Zaro, “The automated computation of tree-level and next-to-leading order differential cross sections, and their matching to parton shower simulations,” *JHEP* **07** (2014) 079, [arXiv:1405.0301 \[hep-ph\]](https://arxiv.org/abs/1405.0301).
- [15] R. Frederix, S. Frixione, V. Hirschi, D. Pagani, H. S. Shao, and M. Zaro, “The automation of next-to-leading order electroweak calculations,” *JHEP* **07** (2018) 185, [arXiv:1804.10017 \[hep-ph\]](https://arxiv.org/abs/1804.10017). [Erratum: JHEP 11, 085 (2021)].
- [16] C. Bierlich *et al.*, “A comprehensive guide to the physics and usage of PYTHIA 8.3,” *SciPost Phys. Codeb.* **2022** (2022) 8, [arXiv:2203.11601 \[hep-ph\]](https://arxiv.org/abs/2203.11601).
- [17] R. D. Ball *et al.*, “Parton distributions with LHC data,” *Nucl. Phys. B* **867** (2013) 244–289, [arXiv:1207.1303 \[hep-ph\]](https://arxiv.org/abs/1207.1303).
- [18] S. Frixione and B. R. Webber, “Matching NLO QCD computations and parton shower simulations,” *JHEP* **06** (2002) 029, [arXiv:hep-ph/0204244](https://arxiv.org/abs/hep-ph/0204244).
- [19] H.-S. Shao, “ J/ψ meson production in association with an open charm hadron at the LHC: A reappraisal,” *Phys. Rev. D* **102** no. 3, (2020) 034023, [arXiv:2005.12967 \[hep-ph\]](https://arxiv.org/abs/2005.12967).
- [20] **LHCb** Collaboration, R. Aaij *et al.*, “Observation of double charm production involving open charm in pp collisions at $\sqrt{s} = 7$ TeV,” *JHEP* **06** (2012) 141, [arXiv:1205.0975 \[hep-ex\]](https://arxiv.org/abs/1205.0975). [Addendum: JHEP 03, 108 (2014)].
- [21] **LHCb** Collaboration, R. Aaij *et al.*, “Measurement of the B^\pm production cross-section in pp collisions at $\sqrt{s} = 7$ and 13 TeV,” *JHEP* **12** (2017) 026, [arXiv:1710.04921 \[hep-ex\]](https://arxiv.org/abs/1710.04921).
- [22] **LHCb** Collaboration, R. Aaij *et al.*, “Measurements of prompt charm production cross-sections in pp collisions at $\sqrt{s} = 13$ TeV,” *JHEP* **03** (2016) 159, [arXiv:1510.01707 \[hep-ex\]](https://arxiv.org/abs/1510.01707). [Erratum: JHEP 09, 013 (2016), Erratum: JHEP 05, 074 (2017)].
- [23] **LHCb** Collaboration, R. Aaij *et al.*, “Production of associated Υ and open charm hadrons in pp collisions at $\sqrt{s} = 7$ and 8 TeV via double parton scattering,” *JHEP*

- 07** (2016) 052, [arXiv:1510.05949 \[hep-ex\]](https://arxiv.org/abs/1510.05949).
- [24] **LHCb** Collaboration, R. Aaij *et al.*, “Associated production of prompt J/ψ and Υ mesons in pp collisions at $\sqrt{s} = 13$ TeV,” *JHEP* **08** (2023) 093, [arXiv:2305.15580 \[hep-ex\]](https://arxiv.org/abs/2305.15580).
- [25] **LHCb** Collaboration, R. Aaij *et al.*, “Precision measurement of the B_c^+ meson mass,” *JHEP* **07** (2020) 123, [arXiv:2004.08163 \[hep-ex\]](https://arxiv.org/abs/2004.08163).
- [26] **BESIII** Collaboration, M. Ablikim *et al.*, “Observation of a Charged Charmoniumlike Structure in $e^+e^- \rightarrow \pi^+\pi^- J/\psi$ at $\sqrt{s} = 4.26$ GeV,” *Phys. Rev. Lett.* **110** (2013) 252001, [arXiv:1303.5949 \[hep-ex\]](https://arxiv.org/abs/1303.5949).
- [27] **Belle** Collaboration, A. Garmash *et al.*, “Observation of $Zb(10610)$ and $Zb(10650)$ Decaying to B Mesons,” *Phys. Rev. Lett.* **116** no. 21, (2016) 212001, [arXiv:1512.07419 \[hep-ex\]](https://arxiv.org/abs/1512.07419).
- [28] A. Ali, Q. Qin, and W. Wang, “Discovery potential of stable and near-threshold doubly heavy tetraquarks at the LHC,” *Phys. Lett. B* **785** (2018) 605–609, [arXiv:1806.09288 \[hep-ph\]](https://arxiv.org/abs/1806.09288).
- [29] **Particle Data Group** Collaboration, S. Navas *et al.*, “Review of particle physics,” *Phys. Rev. D* **110** no. 3, (2024) 030001.

TABLE I. Integrated luminosity required for a 5σ discovery for different T_{bc} parameter assumptions, assuming $\sigma(T_{bc}) = 103$ nb and $\mathcal{B}(T_{bc} \rightarrow B^- D^+) = 0.5$. Both the baseline and conservative maximal-background scenarios are shown.

DPS σ_{eff} [mb]	$m(T_{bc}), \Gamma(T_{bc})$ [MeV]	\mathcal{L}_{int} [fb^{-1}] (NLO SPS 3FNS)	\mathcal{L}_{int} [fb^{-1}] (LO SPS 4FNS, max)
5	7167, 0.5	24 ± 12	25 ± 13
	7167, 5.0	25 ± 13	26 ± 13
	7229, 10	40 ± 20	40 ± 21
	7229, 40	66 ± 33	68 ± 34
15	7167, 0.5	20 ± 10	20 ± 10
	7167, 5.0	21 ± 10	21 ± 10
	7229, 10	26 ± 13	26 ± 13
	7229, 40	35 ± 18	37 ± 19
30	7167, 0.5	19 ± 9	19 ± 10
	7167, 5.0	19 ± 10	20 ± 10
	7229, 10	22 ± 11	23 ± 11
	7229, 40	27 ± 14	29 ± 15

TABLE II. Minimum observable $\sigma(T_{bc}) \times \mathcal{B}(T_{bc} \rightarrow B^- D^+)$ required for a 5σ discovery of T_{bc} at $\mathcal{L}_{\text{int}} = 50 \text{ fb}^{-1}$ (Run 2+Run 3+Run 4) for different T_{bc} parameter assumptions, shown for both the baseline and conservative maximal-background scenarios.

DPS σ_{eff} [mb]	$m(T_{bc}), \Gamma(T_{bc})$ [MeV]	$\sigma(T_{bc}) \times \mathcal{B}$ [nb] (NLO SPS 3FNS)	$\sigma(T_{bc}) \times \mathcal{B}$ [nb] (LO SPS 4FNS, max)
5	7167, 0.5	30 ± 11	30 ± 11
	7167, 5.0	31 ± 11	31 ± 12
	7229, 10	43 ± 15	44 ± 15
	7229, 40	60 ± 19	60 ± 19
15	7167, 0.5	23 ± 10	23 ± 10
	7167, 5.0	24 ± 10	24 ± 10
	7229, 10	31 ± 12	31 ± 12
	7229, 40	40 ± 14	41 ± 14
30	7167, 0.5	21 ± 9	21 ± 9
	7167, 5.0	21 ± 10	22 ± 10
	7229, 10	26 ± 11	27 ± 11
	7229, 40	32 ± 12	34 ± 13

TABLE III. Minimum observable $\sigma(T_{bc}) \times \mathcal{B}(T_{bc} \rightarrow B^- D^+)$ required for a 5σ discovery of T_{bc} at $\mathcal{L}_{\text{int}} = 300 \text{ fb}^{-1}$ (Run 2+Run 3+Run 4) for different T_{bc} parameter assumptions, shown for both the baseline and conservative maximal-background scenarios.

DPS σ_{eff} [mb]	$m(T_{bc}), \Gamma(T_{bc})$ [MeV]	$\sigma(T_{bc}) \times \mathcal{B}$ [nb] (NLO SPS 3FNS)	$\sigma(T_{bc}) \times \mathcal{B}$ [nb] (LO SPS 4FNS, max)
5	7167, 0.5	9 ± 3	10 ± 3
	7167, 5.0	10 ± 3	10 ± 3
	7229, 10	15 ± 4	15 ± 4
	7229, 40	21 ± 6	22 ± 6
15	7167, 0.5	6 ± 2	6 ± 2
	7167, 5.0	6 ± 2	7 ± 2
	7229, 10	10 ± 3	10 ± 3
	7229, 40	13 ± 4	14 ± 4
30	7167, 0.5	5 ± 2	5 ± 2
	7167, 5.0	5 ± 2	6 ± 2
	7229, 10	7 ± 2	8 ± 3
	7229, 40	10 ± 3	11 ± 3